Combining functional annotation and multi-trait fine-mapping methods improves fine-mapping resolution at glycaemic trait loci

Jana Soenksen[1,2], Ji Chen[1], Arushi Varshney[3], Susan Martin[1], MAGIC[4], Stephen C. J. Parker[3,5,6], Andrew P. Morris[7,8], Jennifer L. Asimit[9], Inês Barroso[1*]

1 University of Exeter, Exeter Centre of Excellence for Diabetes Research (EXCEED), University of Exeter, Exeter, UK

2 Living Systems Institute, Clinical and Biomedical Sciences, University of Exeter, Exeter, UK

3 Department of Computational Medicine and Bioinformatics, University of Michigan, Ann Arbor, Michigan, US

4 Full MAGIC membership listed in the Supplementary information

5 Department of Human Genetics, University of Michigan, Ann Arbor, Michigan, US

6 Department of Biostatistics, University of Michigan, Ann Arbor, Michigan, US

7 Centre for Genetics and Genomics Versus Arthritis, University of Manchester, Manchester, UK

8 Centre for Musculoskeletal Research, University of Manchester, Manchester, UK

9 MRC Biostatistics Unit, University of Cambridge, Cambridge, UK

* Corresponding author

Abstract

The Meta-Analysis of Glucose and Insulin-related traits Consortium (MAGIC) identified 242 loci associated with glycaemic traits fasting insulin (FI), fasting glucose (FG), 2h-Glucose (2hGlu), and glycated haemoglobin (HbA1c). However, most causal variants remain unknown. We investigated whether combining multi-trait fine-mapping with functional information would improve fine-mapping resolution.

Using single-trait fine-mapping results (FINEMAP) as input, we performed multi-trait fine-mapping (flashfm) at 50 loci significantly associated with >1 glycaemic trait. We considered 32 cell-type specific and 28 static annotations to build enrichment models with fGWAS. We performed annotation-informed fine-mapping, using FINEMAP and flashfm, with resulting prior probabilities.

Compared to annotation-agnostic single-trait fine-mapping, multi-trait fine-mapping reduced median 99% credible set sizes (99% CS) from 58 to 17.5 ($p=5.75 \times 10^{-18}$). Annotation information reduced 99% CS from 67 to 50.5 ($p=1.57 \times 10^{-7}$) in single-trait, and to 14.5 ($p=2.69 \times 10^{-18}$) in multi-trait fine-mapping.

In conclusion, multi-trait and annotation-informed fine-mapping narrow down likely causal variants, separately and combined.

Introduction

Genetic studies of fasting and post-prandial measures of insulin and glucose, and glycated haemoglobin (HbA1c) levels have provided insights into pathways related to glucose homeostasis and diabetes pathophysiology [1-3]. The largest multi-ancestry study from MAGIC (Meta-Analysis of Glucose and Insulin-related traits Consortium) identified 242 loci associated with glycaemic traits fasting insulin (FI), fasting glucose (FG), 2-hour glucose (2hGlu) and HbA1c [1]. The authors demonstrated that multi-ancestry fine-mapping improved resolution compared to single-ancestry fine-mapping when comparing results with equivalent sample sizes [1]. However, fine-mapping could not resolve the majority of the loci to a single causal variant. Recently, fine-mapping methods that leverage information across multiple traits have been developed [4]. In addition, methods that leverage functional annotation have also been shown to improve fine-mapping resolution [5, 6].

Here, we used association results from Chen et al [1] to investigate whether multi-trait fine-mapping would improve fine-mapping resolution by leveraging information across multiple glycaemic traits. We compared the results to single-trait fine-mapping performed in the European (EUR)-like group and to multi-ancestry fine-mapping from Chen et al [1]. In addition, taking advantage of the functional annotations known to be enriched for each of the glycaemic traits [1], we explored whether the addition of this information to both single-trait and multi-trait fine-mapping approaches would help to further improve fine-mapping resolution, and identify the underlying causal variants.

Results

Identification of loci for fine-mapping

Of the 234 loci fine-mapped by Chen et al [1], we focused on 155 loci that were associated (p-value<$5x10^{-8}$) with at least one of the glycaemic traits, FI, FG, HbA1c and 2hGlu, in EUR-like discovery data (**Supplementary table 1 & Supplementary Figure 1**)**.** Of these, two loci near *GCK* and *G6PC2* were excluded because previous fine-mapping had demonstrated multiple independent variants at each locus, and their roles in glucose homeostasis are well-established [7-9]. We noted that three loci associated with FG, 2hGlu and FI overlapped, and given the possibility of shared common causal variant(s), we merged them into a single locus and repeated single-trait fine-mapping for this new larger locus (**Methods**). Of the resulting 151 loci, we took forward for multi-trait fine-mapping, a subset of 50 loci that associated with a second glycaemic trait with p-value<10^{-6} in EUR-like fine-mapping datasets (**Methods**). For annotation-informed single-trait fine-mapping we included all 151 loci (**Supplementary table 1**).

There is no single best metric to compare performance of different fine-mapping approaches and as we do not have the ground truth, we focused on the size of the 99 % credible set (99% CS), and the marginal posterior probability (MPP) of causality of individual variants (**Methods**). Although neither of these metrics guarantee that the causal variant has been captured, shorter 99% CS and higher MPP values provide increased confidence in the fine-mapping results. These metrics are commonly used to assess performance in fine-mapping analyses, as they prioritise smaller sets of variants with higher likelihood of being causal for downstream functional studies. For these reasons, we have chosen to focus on these metrics.

Multi-trait fine-mapping improves resolution compared to single-trait fine-mapping

We used the single-trait fine-mapping results at 50 loci (110 locus-trait associations), as input for multi-trait fine-mapping (**Methods**). When comparing the overall performance of the multi-trait to single-trait fine-mapping, the median size of the 99% CS was reduced from 58 (lower quartile = 13, upper quartile = 246.25) in single-trait to 17.5 (lower quartile = 6, upper quartile = 70.5) variants in multi-trait ($p=5.75 \times 10^{-18}$, **Figure 1 A & C**). All 99% CS sizes either stayed the same or were reduced in multi-trait fine-mapping. Furthermore, the median MPP of the variant with the highest MPP (top variant) significantly increased from 0.324 (lower quartile = 0.167, upper quartile = 0.617) to 0.478 (lower quartile = 0.271, upper quartile = 0.851) in multi-trait fine-mapping ($p=7.13 \times 10^{-8}$, **Figure 1 B**). Overall, multi-trait fine-mapping led to more locus-trait associations with smaller 99% CS sizes compared to single-trait fine-mapping (**Figure 1 C**). For example, the number of locus trait-associations with 1 variant in the 99% CS doubled from 2/110 to 4/110, while those locus traits-associations with 2-5 variants in the 99% CS increased from 7/110 in single-trait fine-mapping to 21/110 in multi-trait fine-mapping (**Figure 1 C**).

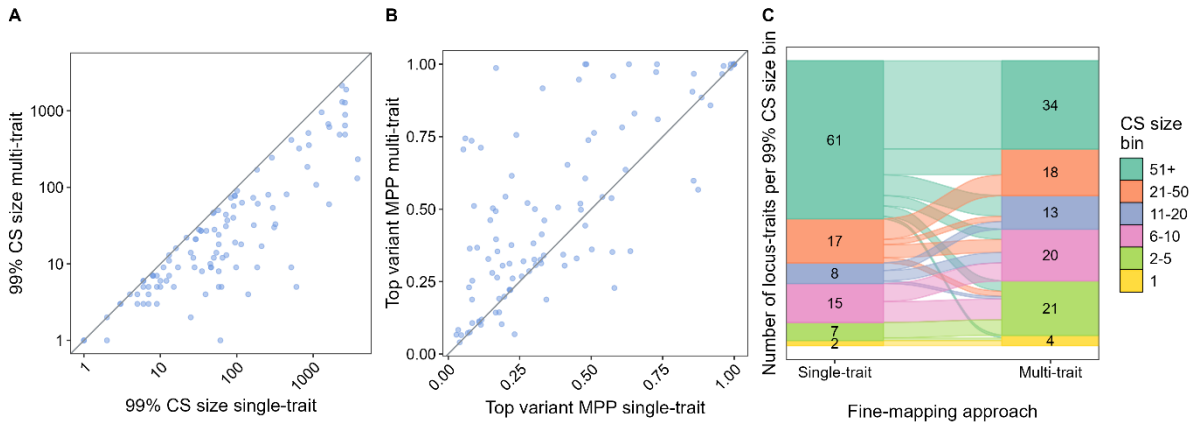

Figure 1 Comparison of multi-trait and single-trait fine-mapping results A&B: *Each dot represents the respective results at a locus-trait association according to the single-trait fine-mapping approach FINEMAP (x-axis) compared to the multi-trait approach Flashfm (y-axis), both are single-ancestry analysis performed in EUR-like populations. The grey line represents the line of equality. Multi-trait results were obtained using the single-trait results as input.* ***A****: Number of SNPs in the 99% CS.* ***B****: Marginal posterior probability (MPP) of the variant with the highest MPP at each locus-trait association.* ***C****: Comparison of the number of locus-trait associations in each 99% CS size bins between different methods (indicated by number in bar chart) and illustrates how the bins of locus-traits change between methods.*

Overall fine-mapping performance is similar for multi-ancestry and multi-trait fine-mapping

Both multi-trait and multi-ancestry fine-mapping can improve fine-mapping resolution compared to single-trait single-ancestry fine-mapping. However, depending on the datasets available multi-ancestry fine-mapping might not be possible. Furthermore, at some loci multi-ancestry fine-mapping performs worse than single-ancestry fine-mapping likely due to effect size heterogeneity between different populations [1]. We compared the resolution of multi-trait fine-mapping with that of multi-ancestry fine-mapping at the subset of 97 locus-trait associations which were also significantly associated in multi-ancestry data (log10BF>6, **Figure 2**). The median 99% CS size of multi-ancestry fine-mapping was 24 compared to 18 in multi-trait fine-mapping (p=0.128, **Figure 2 A & C**). The 99% CS size in multi-trait analysis was reduced in 44 of 97 locus-trait associations (45.4%) compared to multi-ancestry and was the same size in another 12 locus-trait associations. This highlights that in some cases fine-mapping resolution improved compared to multi-ancestry fine-mapping even though the overall difference was not significant (**Figure 2 A**). The median MPP of the top variant was 0.534 in multi-ancestry and 0.461 in multi-trait fine-mapping (p=0.361, **Figure 2 B & D**). Overall, these results show no significant difference in performance of multi-trait and multi-ancestry fine-mapping. The best performing fine-mapping approach varied between locus-trait associations. To understand why multi-trait fine-mapping might outperform multi-ancestry fine-mapping at 44 locus-trait associations, we compared the results between single-trait single-ancestry and multi-ancestry fine-mapping (**Supplementary Figure 2**). Of these locus-trait associations with improved multi-trait fine-mapping, 23/44 had performed worse with multi-ancestry fine-mapping compared to single-ancestry single-trait fine-mapping. However, at 21 locus-trait associations, the multi-trait fine-mapping improved over the already improved multi-ancestry fine-mapping. This showed that multi-trait fine-mapping can outperform multi-ancestry fine-mapping, and suggests that performing multi-trait fine-mapping may be helpful to refine association signals even if multi-ancestry fine-mapping has already been conducted.

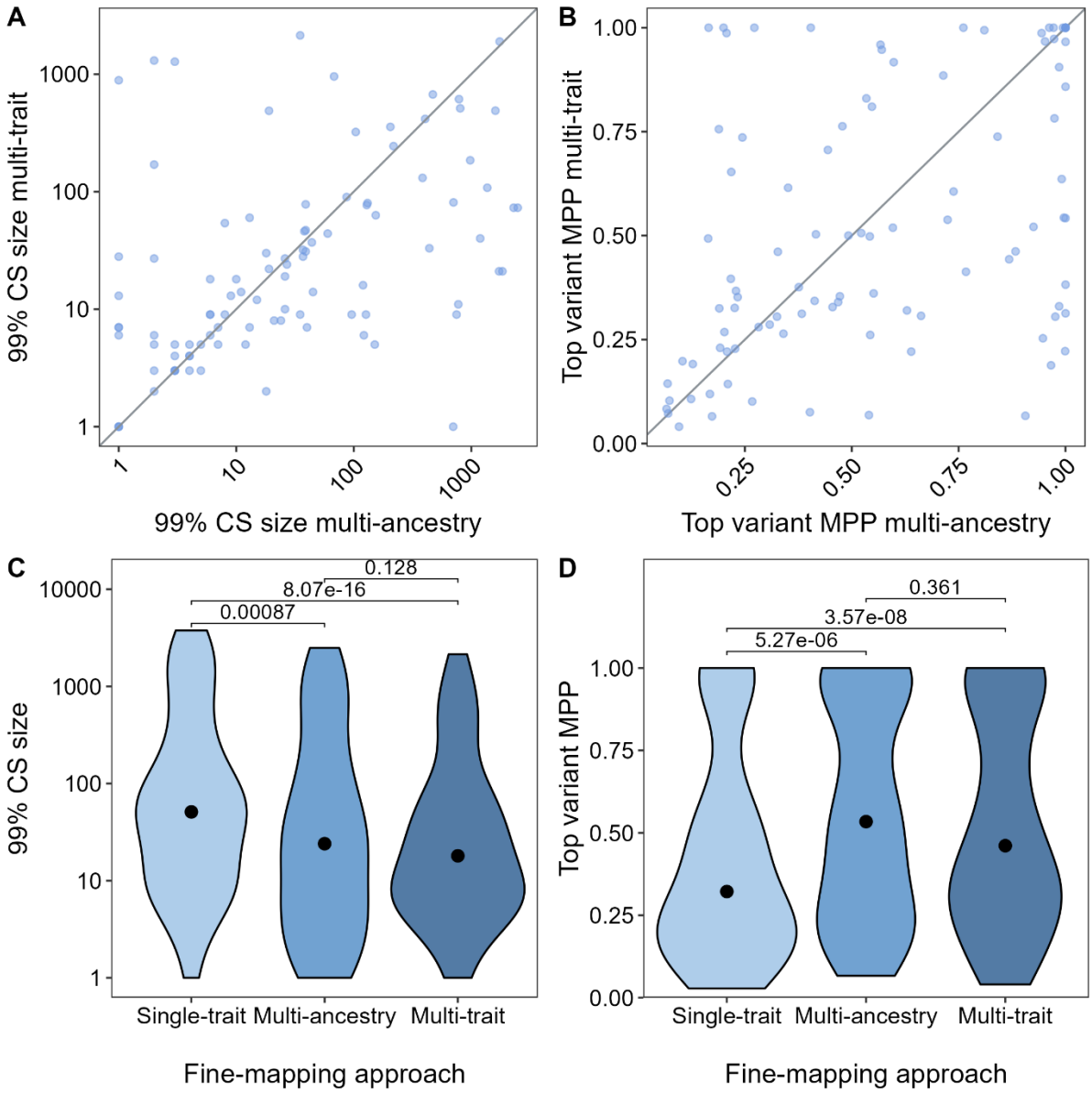

Figure 2 Comparison of agnostic fine-mapping approaches *Multi-trait fine-mapping was carried out with flashfm and using single-trait single ancestry fine-mapping results from EUR-like data obtained with FINEMAP v1.1 as input. Multi-ancestry fine-mapping was carried out using FINEMAP v1.1 in a single trait* ***A&B****: Each dot represents the results at a locus-trait association according to multi-ancestry (x-axis) compared to multi-trait approach (y-axis). The grey line represents the line of equality. The multi-trait results were obtained using the single-trait results from EUR-like as input.* ***C&D****: Includes only locus-trait associations that were analysed with all three approaches. The dot indicates the median, p-values were calculated with a paired two sided Wilcoxon.* ***A&C****: Compares the number of SNPs in the 99% credible set (99% CS).* ***B&D****: The marginal posterior probability (MPP) of the variant with the highest MPP of being causal.*

Annotation-informed multi-trait fine-mapping improves fine-mapping resolution compared to annotation-agnostic and annotation-informed single-trait fine-mapping

So far, all fine-mapping approaches were annotation-agnostic and not informed by any known function of variants. We next sought to explore if using annotation-informed fine-mapping would improve resolution compared to annotation-agnostic single-trait fine-mapping (**Supplementary Figure 3**) and if this could further be improved by conducting annotation-informed multi-trait fine-mapping (**Supplementary Figure 3**).

Starting with the 28 static annotations and 32 cell-type specific stretch enhancers previously analysed by Chen et al [1], we built models of enriched annotations to calculate priors for annotation-informed fine-mapping (**Methods**). The resulting models contained between two (2hGlu) and six annotations (FG and HbA1c, **Supplementary Figure 4**). Static annotations such as coding or conserved regions were included in the final model of multiple glycaemic traits (FG, 2hGlu and HbA1c). FG and 2hGlu results were enriched for islet stretch enhancers, while FI was enriched for adipose-specific stretch enhancers.

After performing annotation-informed fine-mapping using these priors we compared the results with agnostic fine-mapping results (**Methods**). The median 99% CS size decreased significantly from 67 (lower quartile = 20.5, upper quartile = 457.5) variants in agnostic single-trait fine-mapping to 51 (lower quartile = 15.5, upper quartile = 318.5) after adding annotations for the 211 locus-trait associations in EUR-like ($p=6.96 \times 10^{-12}$, **Supplementary Figure 3 A**). Furthermore, there was a significant increase in the median MPP of the top variant from 0.277 in agnostic fine-mapping to 0.418 after adding annotation ($p=6.83 \times 10^{-15}$, **Supplementary Figure 3 C**). Not all locus-trait associations were improved to the same extent. For example, at the *ZBED3-AS1* locus, adding annotations to single trait fine-mapping decreased the 99% CS size more strongly in FG (from 63 to 8 variants) compared to HbA1c (from 15 to 10 variants). At 36 locus-trait associations, adding annotations increased the 99% CS size (**Supplementary Figure 3 A**). However, at a subset of 12 locus-trait associations the MPP of the top variant increased which might suggest the overall fine-mapping did not perform worse at these loci.

We showed that multi-trait fine-mapping and annotation-informed fine-mapping both significantly improved the resolution of the relevant loci. We next combined these two approaches and used annotation-informed fine-mapping on the same subset of 110 locus-trait associations that we had fine-mapped with agnostic multi-trait fine-mapping (**Methods**). The median number of SNPs in the 99% CS decreased from 50.5 (lower quartile = 11.25, upper quartile = 304.75) variants in annotation-informed single-trait fine-mapping to 14.5 (lower quartile = 5.0, upper quartile = 73.5) in annotation-informed multi-trait fine-mapping ($p=2.69 \times 10^{-18}$, **Supplementary Figure 3 B**). The 99% CS size either stayed the same or decreased for all locus-trait associations in multi-trait fine-mapping compared to single-trait fine-mapping. The median MPP of the top variant increased significantly from 0.444 in single-trait to 0.706 in multi-trait fine-mapping ($p = 1.47 \times 10^{-15}$, **Figure 3 A & Supplementary Figure 3 D**).

Of the 110 locus-trait associations, 2 resolved to a single variant in the 99% CS in agnostic single-trait fine-mapping. This improved to 3 in annotation-informed single-trait fine-mapping and 8 in annotation-informed multi-trait fine-mapping (**Figure 3 B**). Furthermore, there were 28 locus-trait associations with 2-5 variants in the 99% CS of with annotation-informed multi-trait fine-mapping, an increase from 6 in the agnostic single-trait fine-mapping results (**Figure 3 B**).

Overall, when comparing fine-mapping results from single-trait agnostic, to single-trait and multi-trait annotation-informed methods there was a gradual improvement of results (**Figure 3 A & B**). However,

188 the 99% CS of some locus-trait associations were not decreased by adding functional annotation.
189 Therefore, there isn't a single best performing method and using multiple approaches is required to
190 find the smallest 99% CS.

191

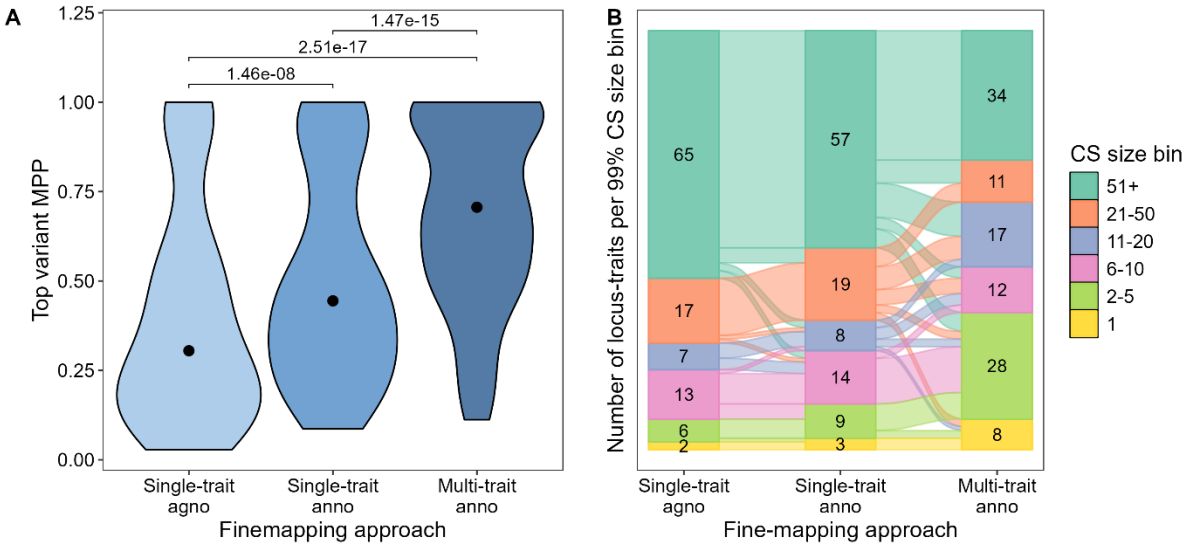

192

193 ***Figure 3 Annotation-informed fine-mapping approaches*** *Single trait fine-mapping was carried out with*
194 *FINEMAP v1.4. Annotation (anno) informed single-trait fine-mapping was carried out using priors calculated with*
195 *fGWAS. Multi-trait annotation-informed fine-mapping was carried out with flashfm using single-trait*
196 *annotation-informed results as input.* ***A*** *The marginal posterior probability (MPP) of the variant with the highest*
197 *MPP of being causal. The dot indicates the median, p-values were calculated with a paired two-sided Wilcoxon.*
198 ***B:*** *Compares the number of locus-trait associations in 99% credible set (99% CS) size bins between different*
199 *methods (indicated by number in bar chart) and illustrates how the bins of locus-traits change between methods*

200

201 # Discussion

202

203 In this study, we aimed to investigate multiple fine-mapping approaches, including multi-trait and
204 functionally informed fine-mapping, and assess their impact on fine-mapping resolution at glycaemic
205 trait loci. Firstly, we applied multi-trait fine-mapping at loci associated with more than one trait. This
206 significantly improved fine-mapping resolution and led to 99% CS sizes either staying the same or
207 decreasing compared to fine-mapping in EUR-like only data. Multi-trait fine-mapping resolution was
208 not significantly different to results obtained from multi-ancestry fine-mapping. Secondly, we used
209 annotation-informed single-trait and multi-trait fine-mapping which led to an overall significant
210 decrease of 99% CS sizes.

211 There was no significant difference between the performance of multi-trait and multi-ancestry fine-
212 mapping approaches. This highlights that multi-trait fine-mapping can be a good alternative to multi-
213 ancestry fine-mapping if data from diverse ancestries is not available. Furthermore, performing both
214 alongside each other can improve fine-mapping for individual locus-trait associations, especially for
215 loci that performed worse in multi-ancestry single-trait fine-mapping compared to single-ancestry
216 single-trait fine-mapping. Multi-ancestry fine-mapping might perform worse due to effect size
217 heterogeneity between ancestries, due to differences in the linkage disequilibrium (LD), or

interactions between genes and environment. However, one limitation of our study was that the sample sizes in the multi-ancestry fine-mapping and the multi-trait fine-mapping were not matched so some of the improvements in multi-ancestry fine-mapping could additionally be driven by increased power due to overall larger sample size.

Adding annotations to single-trait fine-mapping significantly improved the overall fine-mapping resolution, but in some cases adding annotations increased the CS size. This demonstrates the value of performing fine-mapping unbiased by current functional knowledge of the genome. If the true causal variant does not map to one of the annotations included in the model or its function is not known at all, adding annotation information might worsen the performance of fine-mapping at this locus as it might give higher MPPs to non-causal but annotated variants with a higher prior probability. This explains some of the increased 99% CS sizes after adding annotations.

Relatedly, at the *ZBED3-AS1* locus associated with HbA1c, fine-mapping produced smaller 99% CS sizes with all agnostic fine-mapping approaches compared to using the same approaches when fine-mapping the locus when associated with FG. Conversely, the annotation-informed fine-mapping methods led to smaller 99% CS sizes for FG than HbA1c. A potential explanation is that the fGWAS model for FG includes introns as enriched while the HbA1c model does not contain introns. All three variants in the 99% CS of FG are intronic variants of *ZBED3-AS1* and these three variants are also included in the 99% CS of HbA1c. Since the final HbA1c enrichment model does not contain intronic variants these had a lower prior than those in FG. The differences between the annotation models likely affected the extent of the decrease in 99% CS. Functional evidence at this locus supports the causal variant at this locus being the intronic variant rs7732130; Miguel-Escalada et al [10] identified the rs7732130 as being part of an enhancer hub using islet promoter capture Hi-C interaction data. CRISPRa and CRISPRi perturbation of one of these variants, rs7732130 (MPP=0.873), led to gene expression changes of *ZBED3, snoRA47, ZBED3-AS1, PDE8B* and *WDR41* [10]. *ZBED3-AS1* has been shown to regulate *ZBED3* expression which in turn affects Wnt/beta catenin signalling pathway and adipocyte differentiation [11]. *ZBED3* also supressed insulin induced phosphorylation of the insulin receptor and Akt [12]. These pathways can all have an effect on glucose metabolism which is reflected in elevated glucose levels in a mouse knock-out model of *Zbed3* [13]. Given the functional evidence and mechanism linking the 99% CS variant rs7732130 to glucose metabolism via *ZBED3* expression, annotation-informed fine-mapping likely prioritised the right variant for both FG and HbA1c associations at the locus.

In conclusion, for loci associated with multiple traits, conducting multi-trait fine-mapping improved resolution with or without adding annotations. If multi-ancestry fine-mapping is not available or did not improve fine-mapping at a locus, carrying out multi-trait fine-mapping can be a valuable alternative. Finally, adding annotations improved overall fine-mapping resolution but if the causal variant is not part of one of the annotations in the final model it can lead to worse results. Therefore, it is important to consider both agnostic and annotation-informed approaches to find the most likely causal variant.

Data availability

Fine-mapping results (99% credible sets) will be available from the Downloads page of the Common Metabolic Disease Knowledge Portal (cmdkp.org) and the MAGIC website (https://www.magicinvestigators.org/).

Code availability

Code will be available through Zenodo.

262 # Acknowledgements
263 This work was supported by "Expanding excellence in England" award from Research England (IB, JS).
264 IB is funded by Wellcome (227897/Z/23/Z). JLA was supported by UK Medical Research Council
265 (MR/R021368/1, MC_UU_00002/4). This work was also supported by the National Institute for Health
266 and Care Research Exeter Biomedical Research Centre. The views expressed are those of the authors
267 and not necessarily those of the NIHR or the Department of Health and Social Care (IB, JS, JC, SM).

268 # Author contributions
269 IB had the overall responsibility for the project. IB, JLA and APM were involved in project
270 conceptualisation and supervision. JS, APM, JLA and IB drafted the manuscript. AV, SCJP and MAGIC
271 provided data resources. JS, JC and SM were involved in data analysis. JS, AM, JLA and IB interpreted
272 the data. All authors read, edited and approved the final version of the manuscript.

273 # Competing interests
274 The authors declare no competing interests.

275 # Methods

276 ## Genetic and genomic functional annotation datasets used
277 We used trans-ancestry (here called multi-ancestry) and European ancestry (here called EUR-like)
278 meta-analysis summary statistics from MAGIC (http://magicinvestigators.org/downloads/). As per
279 Chen et al [1], cohorts that were only genotyped in the metabochip were excluded from fine-mapping
280 analysis and FG, 2hGlu and FI were adjusted for BMI (**Supplementary table 2**).

281 For analysis of enriched functional annotations, we used static annotations from Finucane et al [14]
282 and cell-type specific annotations, i.e. stretch enhancers from Varshney et al [15] as described by Chen
283 et al [1].

284 ## Locus selection for multi-trait fine-mapping
285 Loci were selected for multi-trait fine-mapping if they were genome-wide significantly associated in
286 the discovery data set ($p<5x10^{-8}$, including metabochip data, **Supplementary table 1**) with at least one
287 of the glycaemic traits, FI, FG, 2hGlu or HbA1c in EUR-like individuals (210 locus-trait associations),
288 based on results from MAGIC [1]. We excluded from fine-mapping loci that were not genome-wide
289 significant in multi-ancestry meta-analysis or if they mapped to the X chromosome. In agreement with
290 recommendations from multi-trait fine-mapping method flashfm [4], we also selected additional loci
291 if they met the suggestive threshold $p<10^{-6}$, with a second trait in the fine-mapping data set. As in
292 Chen et al [1], the fine-mapping data-set did not include cohorts that were only genotyped with the
293 metabochip to avoid biasing results (**Supplementary table 1**).

294 Three loci *DPYSL5*, *GCKR* and *BRE* on chromosome 2 (coordinates chr2:26,640,022-27,677,428,
295 chr2:27,230,940-28,242,603 and chr2:27,768,742-28,768,742) had overlapping coordinates
296 suggesting shared causal variant(s). We merged them into a single locus *DPYSL5;GCKR;BRE*
297 (coordinates chr2:26,730,940-29,268,742) and repeated single-ancestry fine-mapping.

298 ## Reinserting key variants removed due to QC
299 Before performing multi-trait fine-mapping we first performed fine-mapping at 44 locus-trait
300 associations where specific variants had previously been excluded from the analysis due to ancestry
301 specific QC issues. As lead and index variants have a high probability of being causal due to high
302 association evidence, we re-ran single-trait single-ancestry fine-mapping at 15 locus-trait associations

303 at which index variants or top model variants were missing from any trait by including these variants
304 back into the analysis for all traits associated with this locus (**Supplementary table 3**). Furthermore,
305 multi-trait fine-mapping can only include variants present for all traits. To avoid the combination of
306 variants (i.e. model) with the highest posterior probability (PP) of being causal being removed for some
307 locus-trait associations, we also reinserted the top model variants from each of the traits associated
308 with a locus into all of the other traits if not already present. Additionally, we repeated multi-ancestry
309 fine-mapping at 29 locus-trait associations after re-inserting index and lead variants as well as EUR-
310 like top model variants if the MPP was bigger than 0.8 in the same trait (**Supplementary table 3**). Four
311 additional multi-ancestry locus-trait associations were missing EUR-like top model variants but were
312 not rerun because either the likely causal gene at this locus was already identified (*PPARG/SYN2*,
313 *TCF7L2, HFE*) or it was likely to affect HbA1c through non-glycaemic pathways (*SPTA1 (*and *HFE)*).

314 Single-trait fine-mapping with FINEMAP

315 After reinserting variants (see above), a shotgun stochastic search was carried out with FINEMAP v1.1
316 as in Chen et al [1]. Most parameters were kept as the default, except *--corr-config* was set to 0.9 and
317 *--regions* to 1, to match the parameters used in Chen et al [1]. The maximum number of causal variants
318 n_c of each run was iteratively increased until the highest Bayes factor was achieved for n_c-1 and the
319 final version was run with n_c-1 causal variants of the previous run i.e. the final version was run with
320 the maximum number of causal variants set to the number of causal variants that had previously
321 achieved the highest Bayes factor.

322 Multi-trait fine-mapping with flashfm

323 Flashfm (Hernández et al 2021) was used to perform multi-trait fine-mapping. Flashfm uses results
324 from single-trait fine-mapping as input. Therefore, to conduct multi-trait fine-mapping single-trait
325 fine-mapping results from FINEMAP [1] were used.

326 Flashfm requires allele frequencies and effect sizes, which were taken from METAL results generated
327 in Chen et al [1]. If FINEMAP and METAL defined different alleles as the reference allele, the frequency
328 and effect sizes were adjusted to the FINEMAP reference allele. Up to four LD matrices were available
329 for each locus, one for each associated trait. They were based on the subset of people that had the
330 respective trait measured. Since not all trait measures were available for all individuals, the four
331 matrices are based on different people and different sample sizes. For each locus, we used the LD
332 matrix corresponding to the trait with the largest sample size that was also significantly associated
333 with the locus. The LD matrix was converted to a covariance matrix using the reference allele
334 frequency of the trait with the largest sample size. The flashfm parameters were left as the default
335 apart from the odds of sharing between traits which was set to 80% (TOdds=0.25), to reflect the likely
336 increased sharing of causal variants between related glycaemic traits.

337 Functional enrichment analysis with fGWAS

338 For functional enrichment analysis, we considered the 60 annotations used by Chen et al [1] for all
339 traits. We built a model of enriched annotations using fGWAS as described in Mahajan et al [16] and
340 followed the suggested workflow of Pickrell [17]. For each trait we, started by determining the
341 enrichment of all 60 annotations individually; annotations were defined as significantly enriched or
342 depleted if the ln[parameter estimate] and corresponding 95% confidence interval were above or
343 below zero, respectively. Of the significant annotations, we then selected the one with the highest
344 natural logarithm of the maximum likelihood estimate of the enrichment parameter (llk) and added
345 all remaining significant annotations in turn. Of these, we again selected the combination of
346 annotations with the highest llk and kept adding all remaining significant annotations until none
347 increased the llk. To avoid overfitting, we tested different cross-validation penalties in 0.05 increments

348 and selected the one with the highest cross validation likelihood (cross-llk). We then dropped each of
349 the annotations in the model in-turn while applying the cross-validation penalty and checked if any of
350 the reduced models had an increased cross-llk. If so, the annotation was dropped and the process
351 repeated until the highest cross-llk was reached and all estimates were significantly enriched
352 according to their confidence interval. The remaining annotations and their estimates were then used
353 to inform fine-mapping priors.

354 Calculating variant priors for annotation-informed fine-mapping

355 We used the enrichment estimate of the parameters under the penalised likelihood (i.e. β) from the
356 final model obtained from fGWAS as described above to calculate the priors for each SNP included in
357 the fine-mapped loci. The prior for variant *i* is proportional to Q_i

$$Q_i = \prod_{j=1}^{a} \exp\left(\beta_j \times x_{ij}\right) \qquad \textit{Equation 0-1}$$

358 where *a* is the total number of annotations, β_j is the enrichment estimate of annotation *j* and x_{ij} is an
359 indicator variable that takes 1 if variant *i* falls within annotation *j* and 0 if it does not.

360 The rescaled prior of variant *i* (P_i) can then be calculated with

$$P_i = \frac{Q_i}{\sum_{i=1}^{t} Q_i} \qquad \textit{Equation 0-2}$$

361 where *t* is the total number of variants at the locus.

362 Single-trait annotation-informed fine-mapping

363 Chen et al [1] had used FINEMAP v1.1 for fine-mapping but only FINEMAP v1.4 allows for the addition
364 of priors for each variant. To have a fair comparison of results, we reran the single-trait agnostic fine-
365 mapping with FINEMAP v1.4 while keeping all the parameters the same. The default for parameter --
366 *n-conv-sss* was 1000 in FINEMAP v1.1, but the new default in v1.4 is now set at 100. To keep all
367 parameters the same, we changed this back to 1000. The maximum number of causal variants was set
368 to the number determined by Chen et al [1] or to the maximum Bayes factor as determined with
369 FINEMAP v1.1 for the rerun locus-trait associations. We carried out annotation-informed fine-
370 mapping with FINEMAP v1.4 by providing it with the priors from fGWAS. The parameters and
371 maximum number of causal variants were set as for the single-trait fine-mapping with FINEMAP v1.4.

372 Multi-trait annotation-informed fine-mapping

373 For combined multi-trait annotation-informed fine-mapping we used the annotation-informed output
374 from FINEMAP v1.4 as input for flashfm as detailed in Multi-trait fine-mapping with flashfm.

375 Output parameters from fine-mapping results

376 For all fine-mapping results, we constructed 99% credible sets (99% CS) by summing up all models
377 (containing one or more variants) from the largest to the smallest until they reached 99% posterior
378 probability (PP) of containing or tagging the causal variants. The 99% CS size corresponds to the
379 number of distinct variants in the 99% CS. Flashfm and FINEMAP calculate the marginal posterior
380 probabilities of inclusion (MPP) of variants, which is the likelihood that a specific variant is causal or
381 needed to tag the causal variant. This measure can take values between 0 and 1 with 1 indicating the
382 variant has a 100% probability of being or tagging the causal variant.

Data manipulation, visualisation and statistics

Data manipulation, visualisation and statistics were carried out in R [18]. The tidyverse [19] was used for data manipulation. The packages ggpubr [20] “ggsci” [21] , “RColorBrewer” [22], and “VennDiagram” [23] were used to generate figures. We used a two-sided paired Wilcoxon test from the package “rstatix” [24] to calculate p-values.

References

1. Chen, J., et al., *The trans-ancestral genomic architecture of glycemic traits.* Nature Genetics, 2021: p. 1-21.
2. Williamson, A., et al., *Genome-wide association study and functional characterization identifies candidate genes for insulin-stimulated glucose uptake.* Nature Genetics, 2023. **55**(6): p. 973-983.
3. Broadaway, K.A., et al., *Loci for insulin processing and secretion provide insight into type 2 diabetes risk.* The American Journal of Human Genetics, 2023. **110**(2): p. 284-299.
4. Hernández, N., et al., *The flashfm approach for fine-mapping multiple quantitative traits.* Nature Communications, 2021. **12**(1): p. 6147.
5. Weissbrod, O., et al., *Functionally informed fine-mapping and polygenic localization of complex trait heritability.* Nature Genetics, 2020. **52**(12): p. 1355-1363.
6. Li, Y., et al., *Funmap: integrating high-dimensional functional annotations to improve fine-mapping.* medRxiv, 2024: p. 2024.06.25.24309459.
7. Downie, C.G., et al., *Multi-ethnic GWAS and fine-mapping of glycaemic traits identify novel loci in the PAGE Study.* Diabetologia, 2022. **65**(3): p. 477-489.
8. Mahajan, A., et al., *Identification and functional characterization of G6PC2 coding variants influencing glycemic traits define an effector transcript at the G6PC2-ABCB11 locus.* PLoS Genet, 2015. **11**(1): p. e1004876.
9. Overway, E.M., et al., *Nonsynonymous single-nucleotide polymorphisms in the G6PC2 gene affect protein expression, enzyme activity, and fasting blood glucose.* Journal of Biological Chemistry, 2022. **298**(2).
10. Miguel-Escalada, I., et al., *Human pancreatic islet three-dimensional chromatin architecture provides insights into the genetics of type 2 diabetes.* Nat Genet, 2019. **51**(7): p. 1137-1148.
11. Xu, H., et al., *Lnc13728 facilitates human mesenchymal stem cell adipogenic differentiation via positive regulation of ZBED3 and downregulation of the WNT/β-catenin pathway.* Stem Cell Research & Therapy, 2021. **12**(1): p. 176.
12. Jia, Y., et al., *Zinc-finger BED domain-containing 3 (Zbed3) is a novel secreted protein associated with insulin resistance in humans.* Journal of Internal Medicine, 2014. **275**(5): p. 522-533.
13. Wu, Y., et al., *Zinc finger BED-type containing 3 promotes hepatic steatosis by interacting with polypyrimidine tract-binding protein 1.* Diabetologia, 2024. **67**(10): p. 2346-2366.
14. National Academies of Sciences, E.a.M., et al., *The National Academies Collection: Reports funded by National Institutes of Health*, in *Using Population Descriptors in Genetics and Genomics Research: A New Framework for an Evolving Field*. 2023, National Academies Press (US): Washington (DC).
15. Varshney, A., et al., *Genetic regulatory signatures underlying islet gene expression and type 2 diabetes.* Proc Natl Acad Sci U S A, 2017. **114**(9): p. 2301-2306.
16. Mahajan, A., et al., *Fine-mapping type 2 diabetes loci to single-variant resolution using high-density imputation and islet-specific epigenome maps.* Nat Genet, 2018. **50**(11): p. 1505-1513.
17. Pickrell, J.K., *Joint analysis of functional genomic data and genome-wide association studies of 18 human traits.* Am J Hum Genet, 2014. **94**(4): p. 559-73.
18. R Development Core Team, *R: A language and environment for statistical computing*. 2022, R Foundation for Statistical Computing: Vienna, Austria.
19. Wickham, H., et al., *Welcome to the tidyverse*. 2019: Journal of Open Source Software. p. 1686.
20. Kassambara, A., *ggpubr: 'ggplot2' Based Publication Ready Plots*. 2022.
21. Xiao, N., *ggsci: Scientific Journal and Sci-Fi Themed Color Palettes for 'ggplot2'*. 2018.
22. Neuwirth, E., *RColorBrewer: ColorBrewer Palettes*. 2022.
23. Chen, H., *VennDiagram: Generate High-Resolution Venn and Euler Plots*. 2022.
24. Kassambara, A., *rstatix: Pipe-Friendly Framework for Basic Statistical Tests*. 2022.